J. Fluid Mech. (1985), *vol.* 155, *pp.* 175–191
Printed in Great Britain

A structure for laminar flow past a bluff body at high Reynolds number

By F. T. SMITH

Department of Mathematics, University College London, Gower Street, London WC1E 6BT

(Received 20 August 1984)

The steady planar symmetric motion of an incompressible fluid, past a symmetric bluff body fixed in an otherwise uniform stream, is considered for large Reynolds numbers Re. A laminar-flow structure is proposed which consists primarily of (a) the large-scale flow and (b) the smaller, body-scale, flow. Here (a) involves a pair of massive, effectively inviscid, recirculating eddies set up behind the body and bounded by viscous shear layers. Each eddy has small constant vorticity and its length and width both increase linearly with Re, so that the large-scale potential flow outside the eddies is significantly disturbed from the oncoming stream. This reduces the effective free stream acting on (b). The latter has the Kirchhoff property of a parabolic growth in the eddy width downstream; but its eddy vorticity is non-uniform and substantial, contrary to the Kirchhoff and Prandtl–Batchelor models, and secondary separation is possible. The non-uniform vorticity is provoked by the thick return jet, which is forced back along the centreline in (a) from downstream. Buffer zones, e.g. of length $\propto Re^{\frac{1}{8}}$, are required to join (b) fully to (a). The resulting drag coefficient c_D is believed to be $O(1)$ generally, and is controlled, along with the eddy length and vorticity, by a combination of the viscous–inviscid flow problems posed in both (a) and (b). A special case of small c_D is also covered. The structure seems self-consistent so far, and tends to compare reasonably well with recent numerical solutions of the Navier–Stokes equations at increased Re.

An Appendix describes the inviscid parts of (a) for relatively thin eddies.

1. Introduction

The planar, laminar, separating flow of fluid past a bluff body fixed in an otherwise uniform stream seems central to the understanding of large-scale recirculating eddies, and, despite its tendency to instability, it raises issues of both fundamental and technological concern. Much interest centres on the medium-to-high Reynolds-number (Re) regime, which has been reviewed extensively (e.g. Batchelor 1956; Smith 1979; Fornberg 1980). Many models have been proposed, and seem acceptable on a purely inviscid basis, including the Kirchhoff free-streamline solution, the Prandtl–Batchelor model and variants of these. But the list shortens considerably once viscous effects at large Re are studied, and indeed no model has been shown (yet) to be self-consistent with respect to the Navier–Stokes equations then. In that context the two proposals which have been most seriously considered are those of Kirchhoff and of Prandtl and Batchelor. The former happens to agree well with experimental and numerical findings at medium Re-values (Smith 1979, 1981), but nevertheless it leaves so far unanswered questions about its self-consistency at the closure of the main eddy (Smith 1983). The second proposal (Batchelor 1956) does not agree with experiments or numerical results to date, and no solution of its form has been determined yet for

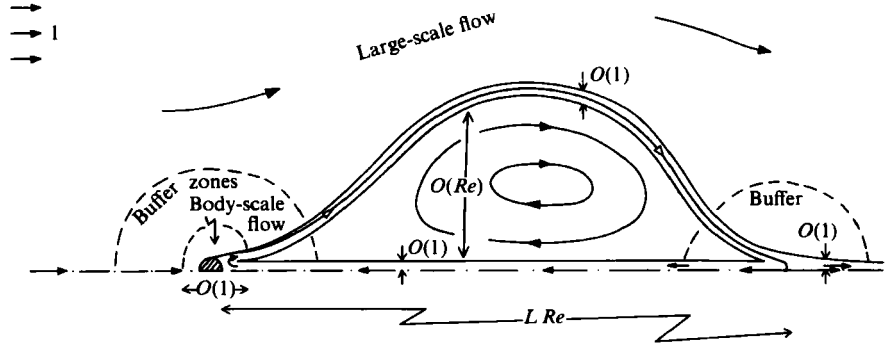

FIGURE 1. Broad structure of the large-Re flow, showing the $O(1)$ body-scale motion, the massive $O(Re)$ large-scale motion concerning the majority of the eddy, and the buffer zones in-between. The dividing streamline is shown by open arrows.

external flow past a smooth body, as far as we know. That does not imply non-existence, of course, and no firm analytical objection has emerged so far; indeed, the Appendix to the present paper tends to suggest that such solutions may exist; but the evidence supporting this proposal seems lacking, especially when viscous effects have to be incorporated. A third proposal (Acrivos *et al.* 1968), based on a viscous eddy downstream, proves inconsistent because of the lack of a significant pressure variation there. The main eddy sizes, length-by-width, predicted in the above three proposals are, in non-dimensional terms, $O(Re)$-by-$O(Re^{\frac{1}{2}})$, $O(1)$-by-$O(1)$ and $O(Re)$-by-$O(1)$ respectively, we note, while the corresponding predicted drag coefficients c_D are $O(1)$, $o(1)$, $O(1)$ in turn.

Recent extensive computations (Fornberg 1985) of the Navier–Stokes equations at higher Re point to an alternative proposal, however, which is the concern of the present work. Fornberg's (1985) results for flow past a circular cylinder suggest an approximately linear increase of both the width and length of the eddy, with increasing Re. The corresponding flow structure for large Re has a massive $O(Re)$-by-$O(Re)$ virtually free eddy and is discussed below (see figure 1). The discussion is based on Sadovskii's (1971) inviscid model (with a free eddy of constant vorticity) and on a tentative study (1977, unpublished) by the present author concerning the validity of that model in the context of viscous effects. The study was tentative because prior to Fornberg's (1985) computations there seemed to be no supportive evidence from numerical solutions of the Navier–Stokes equations. Fornberg's results, however, change that.†

The proposal discussed below for the large-Re structure appears capable of resolving the basic difficulties encountered in previous proposals. In particular, the majority of the eddy has to be even wider than in the extended Kirchhoff proposal (Smith 1979), to generate inviscidly a pressure force sufficient to affect the viscous free shear layer and return centreline wake which bound the eddy. On the other hand the more local, body-scale, flow is not unlike the Kirchhoff form in that its 'open' eddy grows in width parabolically downstream. This is to set up a region of almost-stagnant fluid further downstream, between the thick return wake and the free shear layer, prior to the main eddy flow. Unlike both the Kirchhoff and Prandtl–Batchelor proposals, however, the new account involves a significant non-uniform vorticity in the end of the eddy immediately behind the body, this

† The author is grateful to Mr J. H. B. Smith for pointing out Sadovskii's paper in 1977 and to Dr B. Fornberg for providing a preprint of his (Fornberg 1985) paper.

vorticity being brought about by the return wake's velocity profile and then being convected into the start of the main free shear layer downstream.

Section 2 addresses the large-scale structure associated with the main eddy, discussing in turn the inviscid nonlinear balance between the eddy motion and the outer potential flow; the viscous properties of the free shear layer and the returning centreline wake; and then the ultimate forward-travelling wake beyond. This is to find a first relation between the drag coefficient c_D and the $O(Re)$-scaled eddy length L. Here c_D is expected to be $O(1)$ generally, which (§2) corresponds to an eddy whose length $L_E \sim Re\,L$ and width H_E are both $O(Re)$. The second relation fixing c_D and L follows from §3, where the body-scale motion is considered. It should be mentioned in passing that the slight displacement of the separation in this motion introduces strictly a correction effect $O(Re^{-\frac{1}{16}})$ in the flow field, as in Smith (1979), but below we omit that effect to simplify matters. The reversal of the thick return wake is achieved within the part of the eddy just behind the body, although possibly at the cost of provoking secondary separation (§3). Next, §4 discusses certain buffer regions necessary between the body-scale and large-scale motions, as well as the inviscid turning and splitting of the free shear layer during the eddy closure. Further comments are presented in §5, while an Appendix considers the inviscid portions of the large-scale structure for a relatively thin eddy. The current account does not rule out the previous major proposals of course, by virtue of possible nonuniqueness, but the account does appear to be very promising; it is also broadly in line with Fornberg's (1985) results at higher Re-values. The numerical tasks required to test its validity are set down in the text.

As regards notation, Cartesian coordinates $l(x, y)$ and corresponding velocities $u_\infty(u, v) = u_\infty \boldsymbol{u}$ are taken, for an oncoming uniform stream $(u_\infty, 0)$ and a bluff body whose typical dimension is l. The flow is assumed to be symmetric about the x-axis, and the body is smooth, e.g. a circular cylinder, although non-smooth shapes can also be accommodated. Steady laminar two-dimensional flow is considered, for an imcompressible fluid of density ρ and kinematic viscosity ν, and the large Reynolds number is $Re = u_\infty l/\nu$. The pressure is written $\rho u_\infty^2 p$, with the free-stream pressure taken as zero, and the stream function $u_\infty l\psi$ is zero along the wake centreline. Finally, the Laplacian operator ∇^2 denotes $\partial^2/\partial x^2 + \partial^2/\partial y^2$.

2. The main eddy-scale flow

The massive main eddy has length and width both $O(Re)$ (see figure 2), so that typically here $(x, y)/Re = (X, Y)$ are $O(1)$, and the unknown eddy shape is then $Y = S(X)$, say, for $0 < X < L$. Here the unknown eddy length $L_E = Re\,L$ to leading order. The flow structure consists of three main zones I–III, in all of which p, $|\boldsymbol{u}|$ are typically $O(1)$. The first is the predominantly inviscid outer zone I of fluid emanating from upstream infinity and hence governed by the nonlinear potential-flow problem of motion past, and attached to, the effective body shape $Y = S(X)$, to leading order. The second zone II is the majority of the recirculating eddy, inviscid and so having a uniform unknown vorticity. Third are the thinner viscous regions III, of characteristic thickness $O(1)$ but length $O(Re)$. These are the free shear layer III_1 and the return wake III_2, for $0 < X < L$, which act as vortex sheets bounding the inviscid zone II, while zone III_3 is the ultimate wake extending downstream from the eddy closure point B near $X = L$.

In the structure proposed here we have in mind principally the goal/property of an $O(1)$ drag coefficient c_D, although a small c_D value can also be dealt with later.

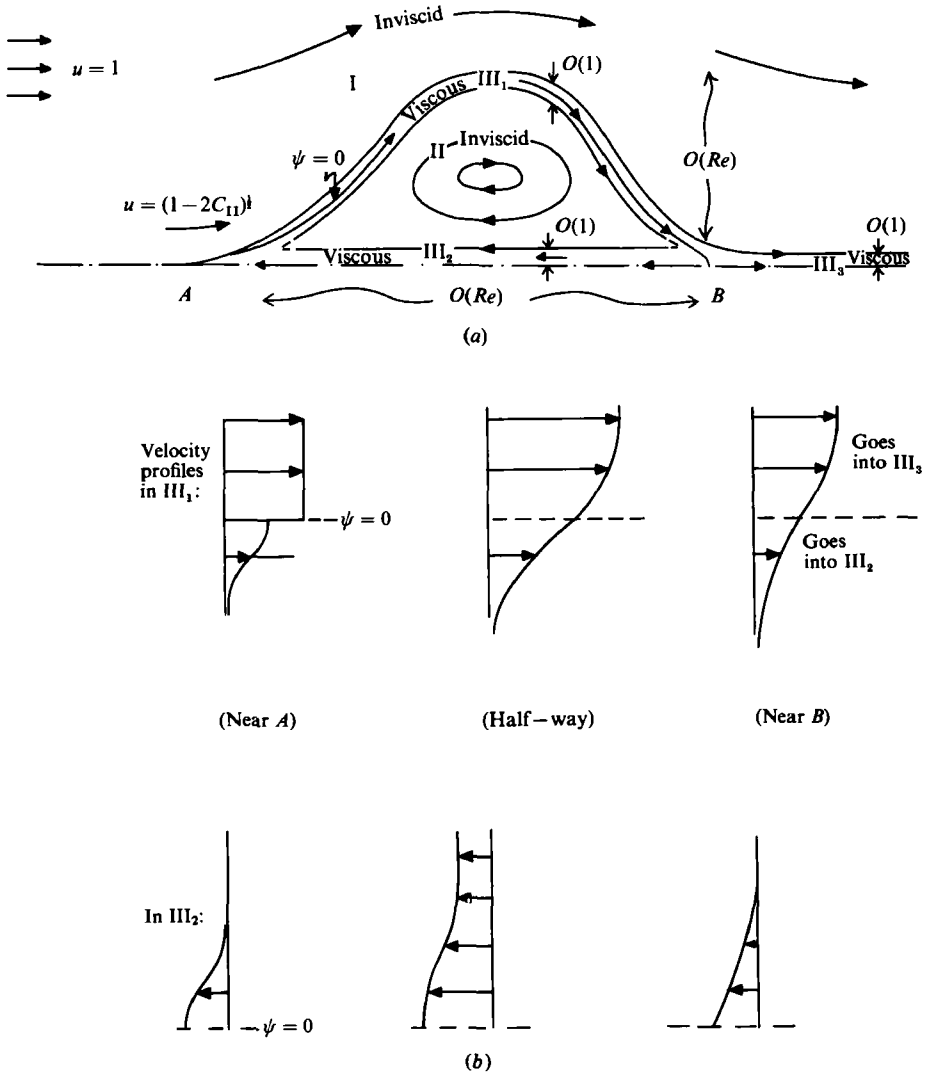

FIGURE 2. (*a*) The large-scale structure, comprising the inviscid $O(Re)$-by-$O(Re)$ zones I and II, of effectively zero and non-zero (constant) vorticity respectively, and the three viscous layers $O(Re)$-by-$O(1)$ denoted $\mathrm{III}_{1,2,3}$. (*b*) Typical velocity profiles for the viscous layers III_1 and III_2.

As a check, a c_D of $O(1)$ requires the mass deficit in the ultimate wake far downstream to be $O(1)$ also, since from the global momentum balance in the Navier–Stokes equations

$$2\int (1-u)\,\mathrm{d}y = c_D, \tag{2.1}$$

the integral here extending across the half-wake $y \geqslant 0$ far downstream (see e.g. Smith 1979). Hence the typical viscous displacement thickness of III_3 must be $O(1)$, and, from continuity through the closure process at B, the same thickness holds for III_1. That requires the typical lengthscale x of III_1, i.e. the eddy dimensions, to be $O(Re)$, to balance inertial and viscous forces, given $|u| = O(1)$. Moreover, the $O(1)$ mass-deficit property also demands III_1 to be a non-trivial zone, a genuine sheet of vorticity

variation, between I and II. So this rather tends to favour the account of Sadovskii (1971), who addresses the purely inviscid problem of the coupling/self-consistency necessary between I and II to ensure continuity of pressure and tangential flow at the boundary $Y = S(X)\pm$. A special case also encompassed by the present structure occurs, with c_D probably small (see also §5), in which there is not a genuine vortex sheet between I and II, i.e. the flow speed is also continuous at $Y = S(X)$, corresponding usually to only a small mass deficit in III_1 and hence in III_3. The inviscid problem in this special limiting case is studied by Pierrehumbert (1980). To be definite, however, let us suppose for the most part that c_D is $O(1)$ in general and take Sadovskii's inviscid model. Further support for the proposition that c_D is $O(1)$ is given in §3 below, with other relevant comments deferred until §5.

2.1. *The inviscid regions I and II*

In I and II the flow solution then expands in the form

$$(\psi, u, p) = (Re\,\overline{\psi}, \bar{u}, \bar{p})\,(X, Y)\,[1 + O(Re^{-1})], \tag{2.2}$$

and so the Navier–Stokes equations reduce to the Euler equations there, to two leading orders at least. Conservation of vorticity therefore yields the governing equations

$$\overline{\nabla}^2\overline{\psi} = \begin{cases} 0 & \text{in I}, \quad (2.3a) \\ -\overline{\Omega} & \text{in II}, \quad (2.3b) \end{cases}$$

with $\overline{\nabla}^2 = \partial^2/\partial X^2 + \partial^2/\partial Y^2$. Here the scaled vorticity constant $\overline{\Omega}$ is unknown, but $O(1)$ and negative, its constancy following from the Prandtl–Batchelor argument for closed streamlines. The unscaled vorticity $-\nabla^2\psi \sim Re^{-1}\overline{\Omega}$. The boundary conditions relevant are, with subscripts I and II relating to the zones I and II in turn,

$$\left.\begin{aligned} \overline{\psi}_{\mathrm{II}} &= 0 \quad (0 < X < L), \\ \overline{\psi}_{\mathrm{I}} &= 0 \quad (X < 0,\ X > L) \end{aligned}\right\} \quad \text{at } Y = 0, \tag{2.3c,d}$$

$$\left.\begin{aligned} \overline{\psi}_{\mathrm{I}} &= \overline{\psi}_{\mathrm{II}} = 0, \\ \bar{p}_{\mathrm{I}} &= \bar{p}_{\mathrm{II}} \end{aligned}\right\} \quad \text{at } Y = S(X), \tag{2.3e,f}$$

$$\overline{\psi}_{\mathrm{I}} \sim Y \quad \text{in the far field.} \tag{2.3g}$$

Sadovskii (1971) gives a small family of numerical solutions of exactly this coupled inviscid problem (2.3) for $\overline{\psi}_{\mathrm{I}}$ and $\overline{\psi}_{\mathrm{II}}$. Although the details shown are perhaps rather sketchy, the results appear to depend on only one parameter, effectively the Bernoulli constant C_{II} at the boundary of zone II or equivalently the vorticity constant $\overline{\Omega}$, for a given length L, as might be expected. Here

$$\bar{p} + \tfrac{1}{2}\bar{q}^2 = \begin{cases} \frac{1}{2} & \text{on the boundary } Y = S(X)+, \\ C_{\mathrm{II}} & \text{on } Y = S(X)-, \end{cases} \tag{2.4a}$$

where $\bar{q} \equiv (\bar{u}^2 + \bar{v}^2)^{\frac{1}{2}}$ is the flow speed and $\bar{v} = -\partial\overline{\psi}/\partial X$. So, in view of (2.3$f$), the jump in (speed)^2 across the shear layer III_1 is $\bar{q}_{\mathrm{I}}^2 - \bar{q}_{\mathrm{II}}^2 = 1 - 2C_{\mathrm{II}}$. Sadovskii's parameter is then $h \equiv 4(1-2C_{\mathrm{II}})/(\overline{\Omega}L)^2$; see also the Appendix.

The symmetry of the eddy shapes computed by Sadovskii agrees with the flow reversibility possible at this inviscid level, while near the endpoints A and B the shapes should have a (distance)$^{\frac{3}{2}}$ form in general. For, if the eddy flow II is to turn back at A or B, $\bar{q}_{\mathrm{II}} \to 0+$, in effect the local flow in I is equivalent inviscidly to that past a detaching vortex sheet, for which the $\frac{3}{2}$ power holds (e.g. J. H. B. Smith 1977; F. T. Smith 1978) given the tangential departure which seems necessary at A and

B inter alia to join with the body-scale flow below. Therefore the velocity and pressure in I near A are finite, with

$$\bar{p}(0,0) = C_{\mathrm{II}}, \quad \bar{u}_{\mathrm{I}}(0,0) = (1-2C_{\mathrm{II}})^{\frac{1}{2}}. \tag{2.4b}$$

Limit properties of interest exist for $C_{\mathrm{II}} \to 0$, giving a linearized potential flow as described in the Appendix, and, secondly, for $C_{\mathrm{II}} \to \frac{1}{2}$, corresponding to Pierrehumbert (1980) but subject to non-uniformities (see Smith 1984) close to the endpoints A and B.

The results of Sadovskii are presented in terms of the normalized variables $[\bar{\psi}_*, X_*, Y_*] \equiv [4\bar{\psi}/|\bar{\Omega}|L^2, 2X/L-1, 2Y/l)$, we note, giving a normalized length of 2 and vorticity -1; but the scaled eddy length L and vorticity $\bar{\Omega}$ remain undetermined of course. Sadovskii's results in fact predict $\partial\bar{\psi}_*/\partial Y_*$ in the far field for a given h-value, i.e. they predict $2/|\bar{\Omega}|L$ (from (2.3g)) for a prescribed C_{II} value (however, see also the Appendix). Thus, even for a given L-value, the solution of the inviscid problem (2.3) still depends on the vorticity $\bar{\Omega}$ and exists for a range of values of $\bar{\Omega}$. To fix $\bar{\Omega}$ and L specifically, we must then move on to viscous effects, as follows.

2.2. *Viscous effects:* regions $\mathrm{III}_{1,2}$

Basically the viscous layers $\mathrm{III}_{1,2}$ now act to determine the value of h, i.e. of $\bar{\Omega}L$, through a 'periodicity' condition of continuity, around the circuit

$$A \to \mathrm{III}_1 \to B \to \mathrm{III}_2 \to A.$$

And the viscous layer III_3 then fixes L, through the ultimate-wake-displacement balance in (2.1), and hence fixes $\bar{\Omega}$, in terms of a given drag c_D; see below. These viscous criteria could well settle matters uniquely, although non-uniqueness is still not impossible.

In the viscous free shear layer III_1 and the return wake III_2 (figure 2) (both of $O(1)$ thickness) the flow solution is

$$(\psi, p) = (\Psi, P) + O(Re^{-1}) \tag{2.5}$$

with the normal coordinate, n say, $O(1)$, but the local streamwise coordinate is $O(Re)$. Hence the vorticity $-\nabla^2\psi$ is $O(1)$ here. The boundary-layer equations hold in III_1 and III_2:

$$Q = \pm\partial\Psi/\partial n, \quad Q\frac{\partial Q}{\partial s} \pm \frac{\partial \Psi}{\partial s}\frac{\partial Q}{\partial n} = -\frac{\partial P}{\partial s} + \frac{\partial^2 Q}{\partial n^2}, \quad 0 = -\partial P/\partial n, \tag{2.6a, b, c}$$

where s stands for the arclength in III_1 (scaled with respect to Re), and $-X$ in III_2, while Q is the effective velocity in the s-direction, i.e. $-u$ in III_2. The match with zones I and II requires

$$P = \bar{p}(X, S(X)) \text{ in } \mathrm{III}_1, \quad \bar{p}(X, 0) \text{ in } \mathrm{III}_2, \tag{2.6d}$$

given (2.6c). The normal boundary conditions on Q and Ψ applying here are respectively to merge III_1 with I and II, to merge III_2 (where $n \equiv y$) with II, and to satisfy the symmetry condition at the centreline:

$$Q \to \left\{ \begin{array}{ll} \bar{u}_{\mathrm{I}}[X, S(X)+] & \text{as } n \to \infty \\ \bar{u}_{\mathrm{II}}[X, S(X)-] & \text{as } n \to -\infty \end{array} \right\} \quad \text{in } \mathrm{III}_1, \tag{2.6e, f}$$

$$\left. \begin{array}{l} Q \to -\bar{u}_{\mathrm{II}}(X, 0-) \quad \text{as } n \to \infty, \\ \dfrac{\partial Q}{\partial n} = \Psi = 0 \quad \text{at } n = 0 \end{array} \right\} \quad \text{in } \mathrm{III}_2. \tag{2.6g, h}$$

The other conditions necessary correspond to the periodicity requirement above. This relies on the dynamics of the smaller-scale zones near A and B considered subsequently, but in anticipation of them we may take the

$$Q\text{-profiles to be continuous through } A, B. \tag{2.6i}$$

This is justified later. The continuity here involves only the lower part ($\Psi < 0$) of III_1 being turned and reversed at $X = L-$ to form the starting profile for the integration along III_2; whereas the starting profile for III_1 at $x = 0+$ has a discontinuous form generally, comprising $Q = \bar{u}_{\mathrm{I}}(0,0)$ for $n > 0$, $Q = -u(0+, -n)$ (evaluated from III_2) for $n < 0$ owing to the turnabout of the profile attained in III_2 at $X \to 0+$ (see figure 2).

It should be remarked here that we are assuming single-structured layers III_1 and III_2 in which fluid moves forward in the s-direction throughout. The alternative of a secondary separation happening on this scale is disregarded for now, although the means for its occurrence is provided by the layer-splitting process described by Van Dommelen (1981) and Elliott, Cowley & Smith (1983), if required. The occurrence would affect, but not wreck, the current scheme of things. Again, it is probable that the return viscous wake III_2 does *not* come to rest as $X \to 0+$ near A, despite the driving velocity $\bar{u}_{\mathrm{II}}$ in (2.6g) doing so. The momentum generated around the circuit $A \to \mathrm{III}_1 \to B \to \mathrm{III}_2$ is virtually certain to leave a jet-like profile in III_2 at the approach to A: a similarity solution, by contrast, is not possible there. This 'leftover' return jet then forms a downstream boundary condition for the body-scale flow discussed in §3 below.

The viscous problem (2.6) is best normalized now, in view of the normalization referred to in §2.1. If

$$[\Psi, Q, P, s, n] = [\tfrac{1}{2}L|\bar{\Omega}|^{\frac{1}{2}}\Psi_*, \tfrac{1}{2}L|\bar{\Omega}|Q_*, \tfrac{1}{4}\bar{\Omega}^2L^2P_*, \tfrac{1}{2}L(1+s_*), |\bar{\Omega}|^{-\frac{1}{2}}n_*], \tag{2.7}$$

then the starred variables satisfy (2.6) still, with subscripts $*$ inserted throughout, and the driving (inviscid) velocities $\bar{u}_*$ in (2.6) then are as determined in Sadovskii (1971). Hence the only parameter active is $|\bar{\Omega}|L$, controlling $\bar{u}_*$, and so the periodicity requirement (2.6i) is expected to fix $|\bar{\Omega}|L$, perhaps uniquely. The necessary numerical solution of (2.6) should be of much interest.

2.3. *Determining* $L(c_D)$

Lastly, and almost separately, one may address the ultimate wake III_3. This fixes L for a given value of c_D as follows. In III_3, where $X > L$, the boundary-layer equations (2.6a–c) apply again, since III_3 is also $O(1)$ thick, with n representing y and $Q = u$ to leading order. The starting profile for III_3 at $X = L+$ is the upper part ($\Psi > 0$) of the free shear layer III_1 at $X = L-$, given again the continuity of vorticity through B (see below). Normalizing as in (2.7) then, we still have the boundary-layer equations for III_3. But the results of §2.2 should fix both Ψ_* in III_1, at $X_* = 1-$ ($X = L-$), and the value of $|\bar{\Omega}|L$. Hence, for III_3, the normalized starting profile at $X_* = 1$ and the subsequent driving velocity $\bar{u}_*$ beyond are both prescribed. These, together with the centreline conditions $\partial Q_*/\partial n_* = \Psi_* = 0$ at $n_* = 0$, are sufficient to determine the normalized solution throughout III_3.

In particular as $s_* \equiv X_* \to \infty$, although III_3 expands slowly like $X_*^{\frac{1}{2}}$, its normalized displacement thickness $\int_0^\infty (2/|\bar{\Omega}|L - Q_*)\,\mathrm{d}n_*$ remains $O(1)$ (Smith 1979) as both $\bar{u}_*$ and Q_* approach the free-stream value $\bar{u}_* = 2/|\bar{\Omega}|L$. So the global balance (2.1) becomes

$$|\bar{\Omega}|^{\frac{1}{2}}L \lim_{X_* \to \infty} \left[\int_0^\infty \left(\frac{2}{|\bar{\Omega}|L} - Q_*\right) \mathrm{d}n_*\right] = c_D, \tag{2.8}$$

in view of the normalization (2.7). Here, however, the integral is known at this stage from the normalized solution in III_3, as is $|\bar{\Omega}|L$ from §2.2. Therefore (2.8) yields a first relation between L and c_D.

This first relation can be found from a single forward integration of the normalized boundary-layer equations for layer III_3, again a necessarily numerical task. The task seems unavoidable, we note, because the driving velocity $\bar{u}_*$ due to zone I ($Y \to 0+$) is non-uniform, increasing between B and downstream infinity; hence the momentum integral (Smith 1979) in the wake III_3 gives

$$\frac{\mathrm{d}}{\mathrm{d}X_*}\left[\int_0^\infty (\bar{u}_* Q_* - Q_*^2)\,\mathrm{d}n_*\right] + \frac{\mathrm{d}\bar{u}_*}{\mathrm{d}X_*}\int_0^\infty (\bar{u}_* - Q_*)\,\mathrm{d}n_* = 0. \tag{2.9}$$

So the ultimate wake displacement for large X_*, required in (2.8), depends significantly on the entire solution in III_3 beyond B, in contrast with the case considered by Smith where $\bar{u}_*$ is constant.

In summary, so far, the following calculations are required in sequence for the determination of the scaled eddy length as a function $L(c_D)$ of the leading-order drag c_D.

1. Solve the inviscid problem (2.3) in normalized form as in Sadovskii (1971) (see also the Appendix).
2. Solve the viscous 'periodic' problem (2.6), normalized, to evaluate $|\bar{\Omega}|L$.
3. Solve the ultimate wake problem, normalized, with (2.6*a–e*), to find L and $\bar{\Omega}$ from (2.8) for a given c_D value.

The flow structure appears so far to be self-consistent, but the normalized calculations proposed above should help settle the issue, uniquely or otherwise. Calculation 2, for instance, seems unlikely to have solutions in the two limits referred to just after (2.4*b*).

The second relation required between L and c_D emerges from the discussion below.

3. The body-scale flow

The body-scale flow, where x, y are broadly $O(1)$, is like that in Smith (1979), with the wake being 'open' when viewed locally; but two extra features are present now. First, the eddy, where $\psi < 0$, is not relatively slow or dynamically negligible to leading order because the return jet left over from layer III_2 above has $O(1)$ thickness and velocity, thus causing a significant eddy motion (see figure 3). Secondly, the match with the eddy-scale flow of §2 requires, from (2.4*b*),

$$u \to (1 - 2C_{\mathrm{II}})^{\frac{1}{2}}, \quad p \to C_{\mathrm{II}} \tag{3.1}$$

in the far field, viewed locally again, for the motion outside the eddy. Therefore the effective mainstream velocity operating for the body-scale flow is reduced significantly from the true free-stream value $u = 1$, the latter being attained only at distances longer than the $O(Re)$ eddy scales.

Given the return-jet profile exactly, we may determine all the features of the body-scale flow and hence fix the drag c_D. But at this stage only the maximum $O(1)$ speed and the normalized shape of the return jet are known, $-u = \frac{1}{2}|\bar{\Omega}|LQ_*(|\bar{\Omega}|^{\frac{1}{2}}y)$, not the exact profile, since §2 specifies $L(c_D)$ and $\bar{\Omega}(c_D)$ only as functions of c_D, via (2.8). The body-scale flow must therefore be solved for varying $\bar{\Omega}$ or L to obtain $c_D(\bar{\Omega})$ as a function of $\bar{\Omega}$. That, combined with (2.8), should pin down both c_D and $\bar{\Omega}$, perhaps uniquely so. More details are as follows.

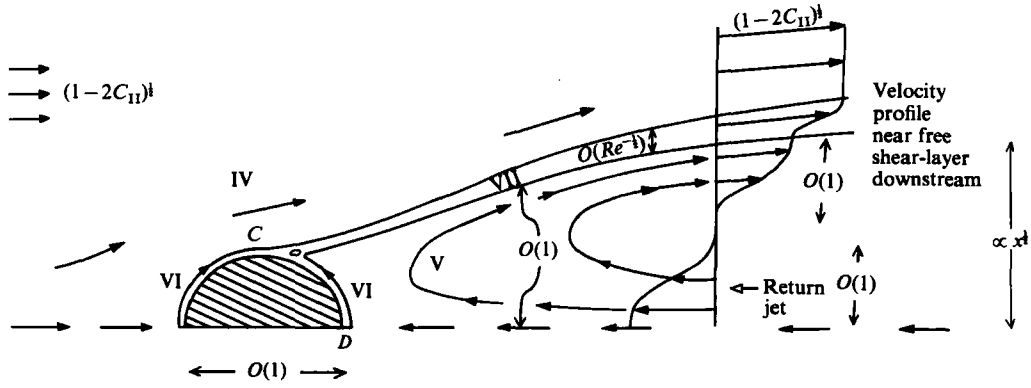

FIGURE 3. Structure of the $O(1)$-by-$O(1)$ body-scale flow, showing main regions IV–VII. The return jet profile $\Psi(0, y)$ indicated is from layer III_2 downstream and is then turned by zone V. Significant secondary separation is neglected.

3.1. *Inviscid zones IV and V*

The body-scale flow has, first, the two effectively inviscid zones IV and V. Here IV is governed by Laplace's equation for ψ with relative error $O(Re^{-\frac{1}{2}})$, and is the continuation of region I of §2. In zone V, which is the upstream end of the eddy, the vorticity-conservation equation holds, V involving the forced continuation and turning by inviscid means of the $O(1)$-thick return jet left over from layer III_2. This return jet is now an acceptable feature of the body-scale flow, unlike in Smith (1979) for example. If $(\psi, p) \sim (\psi_0, p_0) + O(Re^{-\frac{1}{2}})$ for $x, y = O(1)$ then the Navier–Stokes equations yield here

$$\nabla^2\psi_0 = \begin{cases} 0 & \text{in IV}, \quad (3.2a) \\ \mathrm{d}^2\Psi/\mathrm{d}y^2(0+, Y) & \text{in V}, \quad (3.2b) \end{cases}$$

since the profile Ψ in III_2 as $X \to 0+$ fixes the non-uniform vorticity entering V. At first sight, the appropriate boundary conditions are

$$\psi_0 \sim \begin{cases} (1-2C_{II})^{\frac{1}{2}} y & \text{in the far field of IV}, \quad (3.2c) \\ \Psi(0+, y) & \text{as } x \to \infty \text{ in V, for } y = O(1), \quad (3.2d) \end{cases}$$

$$\psi_0 = 0 \quad \text{on the body, on } y = D(x)\pm, \text{ and on the centre-line, in IV and V}, \quad (3.2e)$$

$$p_0 \text{ to be continuous at } y = D(x). \quad (3.2f)$$

Here $y = D(x) + o(1)$ defines the unknown position of the viscous free shear layer dividing IV from V, starting at the separation point C on the body and proceeding (via §4 below) to merge eventually with the start of the free shear layer III_1 further downstream. Further, although secondary separation on the body surface in V may upset the pure tangential-flow condition on the body in (3.2*e*), this is in some sense a secondary issue. It is not disastrous conceptually for the current theme; it is more a nuisance of detail as regards determining $c_D(\bar{\Omega})$. Indeed, it need not necessarily happen (see §3.2). Again, the account of the separation process at point C (fig. 3) is as in F. T. Smith (1979), abetted by J. H. B. Smith's (1977) and F. T. Smith's (1978) showing that the pressure effect in V is negligible there. The process does demand, however, that to leading order

$$\text{the separation at } C \text{ is 'smooth'}, \quad (3.2g)$$

and this also provokes the $O(Re^{-\frac{1}{16}})$ corrections mentioned in §1.

From (3.2*b*, *d*) it is plausible to expect a velocity profile independent of x (apart from a displacement) to emerge just under the shear layer as $x \to \infty$, in V. To conserve vorticity then, from (3.2*b*) and Bernoulli's law,

$$\psi_0 \sim \Psi(0+, D(x)-y) \quad \text{as } x \to \infty \text{ in V, with } D-y = O(1), \tag{3.2h}$$

corresponding exactly to the required turning of the incoming backward jet profile, as assumed in (2.6*i*) previously. Between the incoming and outgoing jets (3.2*d*, *h*) the fluid slows down, for large x in V, ready to latch onto the upstream end of zone II subsequently. Moreover, as noted in §1,

$$D(x) \sim bx^{\frac{1}{2}} \quad \text{as } x \to \infty, \tag{3.3}$$

where the $O(1)$ constant b is related to c_D, similarly to Smith's (1979) case. Thus an $O(1)$ drag, due to the $O(1)$ pressure forces acting on the body, forces b to be $O(1)$ and forces an opening wake on this scale. This opening splits the outgoing profile (3.2*h*) from the incoming one (3.2*d*). The condition (3.3) is also consistent with respect to the far fields of zones IV and V and the momentum balance in zone IV, as in Smith (1979), given the reduced mainstream in (3.2*c*) and (3.1).

The central problem here, then, is to solve (3.2), with the property (3.3). It is a difficult computational problem in general, although limit solutions (Kirchhoff) exist in closed or almost closed form when the eddy motion is relatively slow, for certain body shapes. The solution of (3.2) determines $c_D(\bar{\Omega})$.

3.2. *Viscous effects*

These comprise mainly two traditional $O(Re^{-\frac{1}{2}})$ boundary layers VI (figure 3), one lasting from the front of the body to C, the other going from the rear D of the body to C, according to the proposition above. The former, VI_1, should remain attached under a prescribed favourable pressure gradient until abruptly, around C, it is forced to separate by the triple-deck interaction; more details of this are as in Sychev (1972) and Smith (1979). The second boundary layer, VI_2, however, after being accelerated from D, is subject to a decelerating driving velocity before the clash at C, since C is an inviscid stagnation point. Accordingly, VI_2 cannot both persist in attached form all the way to C and come to rest then. Instead it must either separate at an $O(1)$ distance from C, inducing an $O(1)$-sized secondary separation, or produce a jet-like profile left over at the onset of C. The latter case, where VI_2 stays attached, is possible because the adverse pressure gradient there is not indefinitely large; it is only finitely so (cf. J. H. B. Smith 1977; F. T. Smith 1978).

Which case occurs is dependent largely on the particular body shape, but either case should produce a secondary separation, of small or $O(1)$ extent. A multiple-eddy formation in fact is not impossible. The local secondary separation involving the jet above is described in Smith (1978). The occurrence of secondary separation, however, does not wreck the broad structure proposed, as we have noted before, and it is a matter of calculation (for layers $\mathrm{VI}_{1,2}$) to find out whether the secondary separation is significant or not.

The two boundary layers VI then join, locally or otherwise, to form the $O(Re^{-\frac{1}{2}})$ viscous free shear layer VII. This is driven forward by the slip velocities $u_0(x, D(x)\pm)$ produced in zones IV and V just outside. Its pressure is $p_0(x, D(X))$. Provided the centreline return jet's speed $Q(0,0)$ entering zone V is different from the reduced mainstream speed $(1-2C_{\mathrm{II}})^{\frac{1}{2}}$, the slip velocities above are then unequal, from Bernoulli's theorem in IV and V. So VII expands in thickness as $Re^{-\frac{1}{2}}x^{\frac{1}{2}}$ downstream,

in a Chapman-like similarity form as $x \to \infty$. This eventually merges with the $O(1)$ turned jet-like profile in $(3.2h)$, further downstream (see §4), to form the discontinuous starting profile for layer III_1 already noted in §2.

4. Buffer zones and eddy closure

4.1. *Buffer zones*

One such zone is necessary to convert the parabolic growth of the eddy width emerging from the body-scale flow, in (3.3), to the (scaled distance)$^{\frac{3}{2}}$ growth holding just beyond A in the larger-scale motion of §2. This occurs where $x^{\frac{1}{2}} \sim Re(x/Re)^{\frac{3}{2}}$, i.e.

$$x = O(Re^{\frac{1}{3}}). \tag{4.1}$$

The conversion is a fairly simple affair, however. For the typical eddy width then is $O(Re^{\frac{1}{3}})$, and so its slope is small, $O(Re^{-\frac{1}{3}})$. Hence outside the eddy linearized potential flow properties hold then, while inside the velocity profiles of $O(1)$ thickness associated with $(3.2d, h)$ continue unaltered apart from a displacement effect. The pressure variation induced can be relatively small, with the eddy boundary here being

$$y = Re^{\frac{1}{3}}\left[b\left(\frac{x}{Re^{\frac{1}{3}}}\right)^{\frac{1}{2}} + \bar{b}\left(\frac{x}{Re^{\frac{1}{3}}}\right)^{\frac{3}{2}}\right] \tag{4.2}$$

to keep the eddy pressure at $C_{\mathrm{II}} + o(Re^{-\frac{1}{3}})$ by virtue of the $x^{\frac{1}{2}}, x^{\frac{3}{2}}$ dependence in (4.2). The constant $\bar{b}$ is the coefficient in the starting shape $Y \sim \bar{b}X^{\frac{3}{2}}$ of the large-scale eddy in §2. Little motion takes place in the $O(Re^{\frac{1}{3}})$ by $O(Re^{\frac{1}{3}})$ region lying between the return and forward jets. Again, the displaced viscous shear layer of thickness $O(Re^{-\frac{1}{3}})$ carries on in the Chapman-like form, surrounding the curve (4.2). This form combines with the forward-moving displaced jet $(3.2h)$, of $O(1)$ thickness, at the start of the vortex sheet III_1 as x then increases to $O(Re)$ downstream.

A similar buffer zone is necessary during the eddy-closure process below. Other smaller buffer zones also arise, e.g. close to the separation point at C, just as in Smith (1979), but they have little significance globally.

4.2. *Eddy closure*

The mechanism for the turning near the eddy-closure point B is predominantly inviscid, much like that studied in §3, but simpler owing to the absence of any solid surface (see figure 4). At $O(1)$ distances around B, the shear-layer slope must again become $O(1)$, comparable to its thickness, to induce an $O(1)$ local pressure change sufficient to turn the flow. The governing equations there, for $x - LRe\,(= \tilde{x})$, y of $O(1)$, are in effect

$$\nabla^2\psi = f(\psi) \tag{4.3}$$

again, with $\psi = 0$ on $y = 0$ for symmetry. The local non-uniform vorticity $-f(\psi)$ is prescribed by the incoming displaced profile of the $O(1)$ shear layer III_1 as $X \to L-$, c.f. $(3.2b)$. This profile varies from $(1 - 2C_{\mathrm{II}})^{\frac{1}{2}}$ at its upper extreme to zero underneath. Therefore, to conserve vorticity, exactly the same profile emerges after the closure process, but now split into two, one half going upstream into the start of the return wake III_2, the other half proceeding downstream to form the start of the ultimate wake III_3 (figure 4). A minor viscous sublayer of width $O(Re^{-\frac{1}{3}})$ astride the centreline reduces the vorticity to zero in place of the non-zero value $-f(0)$.

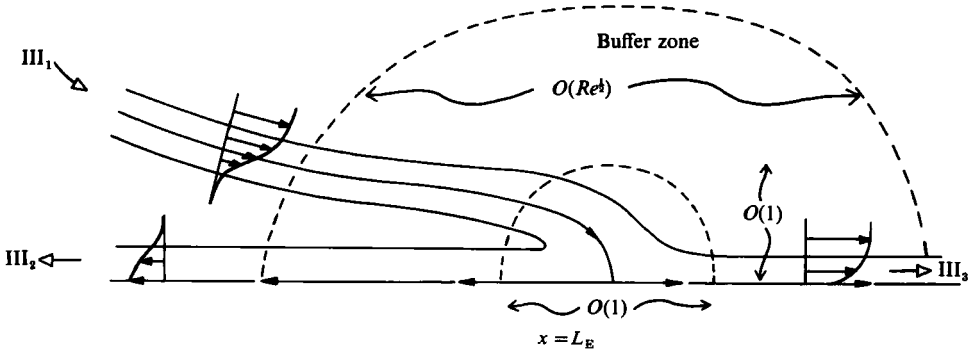

FIGURE 4. The eddy-closure process, including the $O(Re^{\frac{1}{4}})$-length buffer zone. A similar buffer zone is present between the structures of figures 2(*a*) and 3.

The exact turning/splitting above, near B, justifies the assumption (2.6*i*) made earlier, although a computation is required to solve (4.3) entirely; cf. the account of Messiter, Hough & Feo (1973) in a different context. Further, the incoming flow III_1 sits on a curve whose y-positioning grows like $|\tilde{x}|^{\frac{1}{2}}$ as $\tilde{x} \to -\infty$. The one-half power here, like that in (3.3), enables the pressure variation to be negligible, as $\tilde{x} \to -\infty$, thus allowing the flow velocities to become small in the gap between the incoming free shear layer and the outgoing return wake at large negative $\tilde{x}$. This leads on to another buffer region of almost-stagnant fluid lying between, and matching to, the eddy-closure zone described by (4.3) and the main eddy zone II considered earlier. A similar almost-stagnant region occurs near the upstream end of the eddy. These regions may or may not be distinct from the two buffer zones ($Re^{\frac{1}{4}}$-by-$Re^{\frac{1}{4}}$) which control the switch from (distance)$^{\frac{1}{2}}$ to Re(distance/Re)$^{\frac{1}{2}}$ eddy shapes; the buffer near A has been described in §4.1, and the other near B is likewise necessary to join the eddy-closure zone of (4.3) to the main eddy II.

5. Further comments

Certain other details of the flow structure proposed can be worked through, but the new numerical tasks posed already (§§2 and 3) represent the most crucial aspects. These tasks are, first, to pin down an acceptable inviscid solution among those of the Sadovskii kind by solving the viscous problem (2.6) around the eddy boundary (see also Burggraf 1970; Riley 1981); secondly, to solve the normalized ultimate-wake problem (§2.3), thus obtaining a first relation between the drag c_D and the scaled eddy vorticity $\bar{\Omega}$; and, thirdly, to tackle the main body-scale problem (3.2), which yields the required second relation between c_D and $\bar{\Omega}$. The limit calculations entailed here should prove very interesting, and difficult.

These calculations and others posed should also help settle some significant issues arising, such as whether secondary separation occurs or not, and the equality or otherwise of the flow speeds $\bar{q}_{\mathrm{I}}$ and $\bar{q}_{\mathrm{II}}$ at the edges of the free shear layer in the eddy-scale motion. A small amount of suction at the body surface could suppress secondary separation. We note also the absence of secondary separation in Fornberg's (1985) computations so far. But the question associated with $\bar{q}_{\mathrm{I}}$ and $\bar{q}_{\mathrm{II}}$ is a little more involved. So far we have tended to suppose the more general case of Sadovskii (1971), that $\bar{q}_{\mathrm{I}} \neq q_{\mathrm{II}}$, which then corresponds to c_D being $O(1)$ with the eddy dimensions $O(Re)$ generally, in view of the balance (2.1). If the alternative special case $\bar{q}_{\mathrm{I}} = \bar{q}_{\mathrm{II}}$ (Pierrehumbert 1980) holds, however, there are two perhaps rather disquieting or

puzzling features also present. One is that the large-scale eddy becomes increasingly blunt in shape (see Smith 1984) on its approach to the point A representing the body-scale flow. The match with the latter is therefore more involved, with the velocities there being reduced by an order of magnitude. The second feature is that, in line with the reduced velocities near the body, c_D can then be small, with the viscous layers III then being governed by linearized properties invoking displacement effects $o(1)$, from (2.1). Neither feature seems quite as physically sensible or necessary as those associated with the more general case taken above. Although an $O(1)$ value of c_D is still possible in the alternative case if the starting profile for the free shear layer III_1 near A (where $\bar{q}_{\mathrm{I}} = \bar{q}_{\mathrm{II}} \to 0$) is non-zero or non-uniform, the present view rather tends to favour the more general case. We should emphasize nevertheless that as yet the objections to the alternative case are far from firm.

Preliminary comparisons with Fornberg's (1985) results for the Navier–Stokes equations do not seem unfavourable, at higher Reynolds numbers Re. The linear increase of both the eddy length L_{E} and width H_{E}, with increasing Re, emerges approximately for Re above 400 (Fornberg's figures 10, 11) for the circular cylinder. The slopes of H_{E} versus Re and L_{E} versus Re there are about 0.032–0.047 and 0.15 in turn. Their ratio, in the range 0.21–0.31 approximately, then encompasses some of Sadovskii's limiting forms (which hold for $0 < H_{\mathrm{E}}/L_{\mathrm{E}} < 0.293$ approximately; see the Appendix) and Pierrehumbert's case ($H_{\mathrm{E}}/L_{\mathrm{E}} \approx 0.293$). A not dissimilar estimate, but very close to the Pierrehumbert value, is made by Fornberg (private communications, 1984, 1985). Likewise, comparisons concerning the drag c_D, the pressure, and the vorticity in the eddy and in the viscous layers (Fornberg 1984, figures 7–18), can be made. In particular, c_D eventually falls below the Kirchhoff value 0.50 for the circular cylinder at large Re in Fornberg's figure 18: this is in line with the combined drag-reducing effects of the reduced mainstream (3.1) and the $O(1)$ vorticity (3.2b) and increased pressure which act in the eddy, within the body-scale flow. Also, the calculated vorticity and pressure on the cylinder in Fornberg (1980, figures 12, 14) appear not inconsistent with the proposed triple-deck separation (Smith 1979) taking place at a position C downstream of the Kirchhoff value due to the significant eddy motion now included. These comparisons are preliminary, it should be emphasized, and firmer tests must await the limit computations noted.

Subject to those computational studies, however, the flow structure for large Re appears to be self-consistent. It consists principally of the large-scale motion past, within, and around the border of, the massive Re-by-Re eddy, and the body-scale motion of typical $O(1)$ dimensions. These two scales combine to fix c_D and $\bar{\Omega}$, perhaps uniquely. The body-scale motion is not entirely of the Kirchhoff form then, since significant non-uniform eddy vorticity is present there, but it does have the Kirchhoff characteristic of a parabolic widening of the 'open' wake/eddy downstream. This is joined to the (scaled distance)$^{\frac{3}{2}}$ start of the large-scale eddy via a buffer zone. If the structure is correct it could give a great boost to the understanding of many kinds of separation eddies. The dominant feature is that most of the eddy, of size much greater than the body, has significant motion within it, at constant vorticity, and this same feature might be expected to occur in other separating flows. (This is provided the eddy size is not confined deliberately: confinement, as in a driven cavity, in flows through tubes, or in cascade flow, can set up Kirchhoff or Prandtl–Batchelor motions instead, as could non-uniqueness in the present unconfined flow.) The other flows of interest here include non-symmetric ones and the smaller-scale ones associated with thin airfoils, cascade flows or interactive boundary-layer separations (e.g. triple-deck), which more commonly give stable separation eddies in practice. For these smaller-scale

phenomena, moreover, even with the increased likelihood of secondary separation occurring if an eddy totally adjoins a solid surface, the eddy-flow features could well prove more accessible to analysis, as in the Appendix below.

A preliminary version of this paper appeared as Smith (1984); see also Peregrine (1985). The author is grateful to Dr B. Fornberg, Professor N. Riley, Mr J. H. B. Smith, Dr M. J. Werle and the referees for their interest and helpful constructive comments on the problem.

Appendix. Properties of the inviscid problem (2.3), for relatively large negative vorticity

The following analysis points to the properties of solutions for the main large-scale inviscid problem (2.3*a–g*) at the extreme of large negative values of the scaled vorticity $\bar{\Omega}L$, where the constant C_{II} in (2.4*a*) is small. This gives a relatively thin eddy, in contrast with Sadovskii's and Pierrehumbert's results for the thickest eddies obtained at the other extreme, where C_{II} is equal to or numerically close to $\frac{1}{2}$. When $\bar{\Omega}L$ is large and negative we expect the flow solutions in zones I and II to have the form

$$\bar{\psi}_{\mathrm{I}} = Y + O(|\tfrac{1}{2}\bar{\Omega}L|^{-2}), \quad \bar{\psi}_{\mathrm{II}} = |\tfrac{1}{2}\Omega L|^{-3}\tilde{\psi}_{\mathrm{II}} + \ldots, \tag{A 1}$$

with

$$S(X) = \tfrac{1}{2}L|\tfrac{1}{2}\bar{\Omega}L|^{-2}\tilde{S}(X_*) + \ldots, \quad Y = \tfrac{1}{2}L|\tfrac{1}{2}\bar{\Omega}L|^{-2}\tilde{Y} \quad \text{in zone II.} \tag{A 2}$$

Here we use X_* as defined in §2, in place of X, or in effect normalize L to be equal to 2. The orders taken in (A 1) and (A 2) are such that the pressures induced in zones I and II are both typically $O(|\bar{\Omega}L|^{-2})$. The induced pressure in the outside zone I is due to linearized potential flow, while that inside the eddy II is from the thin-layer Euler flow holding there, governed by $\partial^2\tilde{\psi}_{\mathrm{II}}/\partial\tilde{Y}^2 = \frac{1}{2}L$ in view of (A 1), (A 2) and (2.3*b*). Hence

$$\tilde{\psi}_{\mathrm{II}} = \tfrac{1}{4}L(\tilde{Y}^2 - \tilde{Y}\tilde{S}), \tag{A 3}$$

so that from the steamwise momentum balance

$$\bar{P}_{\mathrm{II}} = (\tilde{C} - \tfrac{1}{8}\tilde{S}^2)\,|\tfrac{1}{2}\bar{\Omega}L|^{-2} \tag{A 4}$$

to leading order, where $\tilde{C}$ is an unknown constant. Equating (A 4) to the surface pressure produced by the thin eddy in zone I, we have then the nonlinear integro-differential equation

$$\tilde{C} - \tfrac{1}{8}\tilde{S}^2(X_*) = -\frac{1}{\pi}\int_{-1}^{1}\frac{\tilde{S}'(\xi)\,\mathrm{d}\xi}{(X_* - \xi)} \tag{A 5}$$

for the unknown eddy shape $\tilde{S}(X_*)$, subject to the conditions

$$\tilde{S}(\pm 1) = \tilde{S}'(\pm 1) = 0. \tag{A 6}$$

In (A 5) the Cauchy–Hilbert integral represents a principal value, and the origin of the X_* coordinate is at the eddy centre. The condition in (A 6) of zero slope at the ends of the eddy is required in general for the solutions of (2.3), as noted in §2, in order to match ultimately with the body-scale flow, and it rules out the possibility of the elliptical shape considered by Sychev (1967) and Smith (1979).

The governing equation (A 5) is an integrated form of the Benjamin–Ono equation, for steady flow or nonlinear travelling waves, but with the unusual feature of being confined to a finite interval $|X_*| \leqslant 1$. The author's attempts to solve (A 5) and (A 6) analytically proved inconclusive, and so a numerical approach was adopted. The main difficulty encountered in this was to find a way of avoiding the trivial solution with

$\bar{C}$ and $\bar{S}$ identically zero, on the one hand, and, on the other, the host of solutions with $\bar{S}'(\pm 1)$ infinite, corresponding to locally parabolic eddy shapes near $X_* = \pm 1$, whereas (A 6) requires the cuspidal behaviour $\bar{S} \propto (1-|X_*|)^{\frac{3}{2}}$ as $X_* \to \pm 1$. So we set $\bar{S} = \bar{C}\hat{S}$, assuming $\bar{C}$ to be positive (see below), and integrated (A 5) by parts to obtain formally the equation

$$1-\sigma^2\hat{S}^2 = \frac{1}{\pi}\int_{-1}^{1} \frac{\hat{S}(\xi)\,\mathrm{d}\xi}{(X_*-\xi)^2} \tag{A 7}$$

for $\hat{S}(X_*)$, with the constant $\sigma^2(\equiv \frac{1}{8}\bar{C})$ to be found. Here $\hat{S}$ satisfies (A 6) with $\bar{S}$ replaced by $\hat{S}$. A guess was made for the value of σ and for the $\hat{S}(X_*)$ distribution on a uniform grid in X_* between $X_* = -1$ and $X_* = 1$, with grid size ΔX_*. The left- and right-hand sides of (A 7), effectively the eddy and outside pressures respectively (say $\hat{p}_{\mathrm{II}}$ and $\hat{p}_{\mathrm{I}}$), were then evaluated at each grid point X_*, and the $\hat{S}$-distribution was updated by setting

$$\hat{S}_{\mathrm{new}} = \hat{S}_{\mathrm{old}} + \omega(\hat{p}_{\mathrm{I}} - \hat{p}_{\mathrm{II}}) \tag{A 8}$$

at each X_*, with ω being a positive relaxation factor (typically set as 0.01). The sign of ω here was chosen so that the analogous unsteady equation, with $\partial\hat{S}/\partial t$ in effect added to the left-hand side of (A 7), is stable to short-wavelength effects. The value of σ^2 was also revised at this stage, to enforce the constraints in (A 6), by means of the integral property

$$\pi - \sigma^2 \int_{-1}^{1} \frac{\hat{S}^2(\xi)\,\mathrm{d}\xi}{(1-\xi^2)^{\frac{1}{2}}} = 0 \tag{A 9}$$

derived from integration of (A 7) and inclusion of the end conditions (A 6). The property (A 9) also justifies the earlier assumption that $\bar{C}$ is positive. The latest $\hat{S}_{\mathrm{new}}$ distribution obtained from (A 8) was then used to evaluate the integral in (A 9). Given new values of both $\hat{S}$ and σ^2, therefore, the above process could be repeated, by working out new $\hat{p}_{\mathrm{II}}$ and $\hat{p}_{\mathrm{I}}$ values and reapplying (A 8) and (A 9), and so on. The iterations were continued until the pressure differences $\hat{p}_{\mathrm{II}} - \hat{p}_{\mathrm{I}}$ were reduced to sufficiently small levels, of about 10^{-6}.

All the integrals involved were approximated by a trapezoidal rule. To preserve accuracy in the principal value (A 7) in particular, we subtracted out the singular part of the integrand at $\xi = X_*$ and determined it analytically, thus replacing the right-hand side of (A 7) by

$$\frac{1}{\pi}\int_{-1}^{1} [\hat{S}(\xi) - \hat{S}(X_*) - (\xi - X_*)\hat{S}'(X_*)] \frac{\mathrm{d}\xi}{(X_*-\xi)^2} - \frac{2\hat{S}(X_*)}{\pi(1-X_*^2)} + \frac{\hat{S}'(X_*)}{\pi}\ln\left(\frac{1-X_*}{1+X_*}\right) - (\Delta X_*)\frac{\hat{S}''(X_*)}{\pi} \tag{A 10}$$

and approximating the integral in (A 10) numerically. This part of the procedure was checked by comparisons with analytical results for certain $\hat{S}(X)$ forms satisfying the required cuspidal behaviour at $|X_*| = 1$ (see above), and it stood up well to such tests, despite the very slight irregularity of the integrand in (A 10) as $X_* \to \pm 1$ due to the cusps there. The whole procedure also gave converged results which appeared to conform satisfactorily with first-order accuracy as the grid size was refined, in line nominally with use of the trapezoidal rule. Thus the values obtained for σ were 1.3188, 1.3440, 1.3562 and 1.3621 from the step sizes $\Delta X_* = 0.04, 0.02, 0.01$ and 0.005 in turn, and these extrapolate well linearly to give the estimate

$$\sigma = 1.368 \tag{A 11}$$

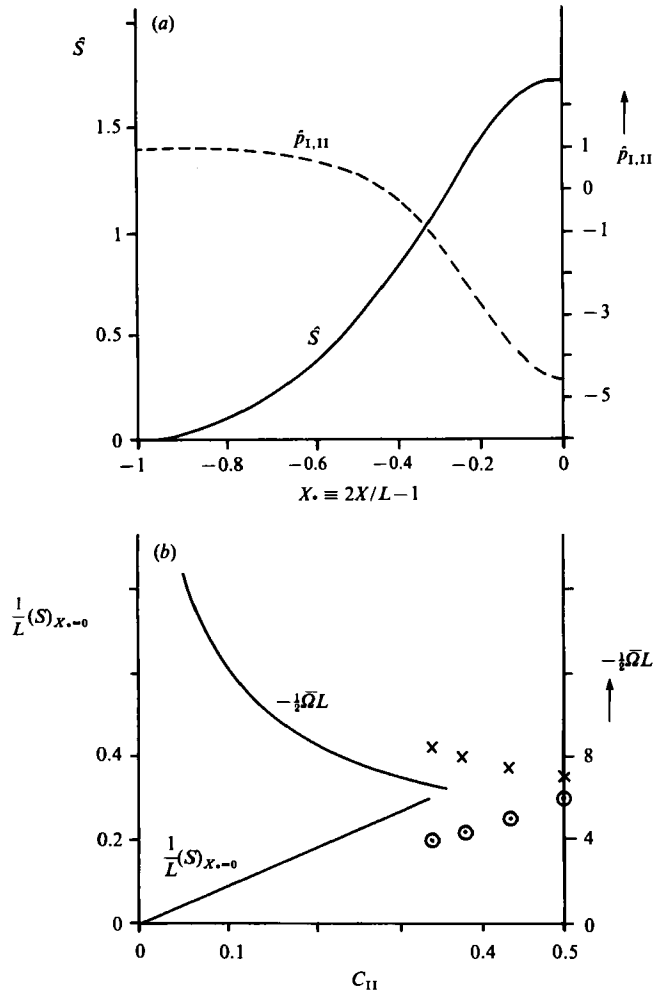

FIGURE 5. (*a*) The numerical solution of (A 5) or (A 7), symmetric about $X_* = 0$, showing the reduced eddy shape $\hat{S}(\equiv \tilde{S}/8\sigma^2)$ and the pressures $\hat{p}_{II} = \hat{p}_I$ (the left-and right-hand sides of (A 7)), versus X_*, where $\sigma \equiv (\frac{1}{6}\tilde{C})^{\frac{1}{4}}$ is given in (A 11). This describes the properties of (2.3) for small values of C_{II} or large $|\bar{\Omega}L|$. (*b*) The inviscid eddy-thickness/length ratio $S(X_* = 0)/L$ and the effective vorticity $\bar{\Omega}L$, versus the Bernoulli constant C_{II}, according to the prediction (A 12) (—) for small C_{II} and to calculated results (⊙, × in turn) read from Sadovskii (1971).

in the limit of zero step size. The full extrapolated solution for $\hat{S}$ and $\hat{p}_I(= \hat{p}_{II})$ is shown in figure 5(*a*). Various starting guesses were made, and all led to the same converged symmetric solution within the limits of accuracy. The solution appears sensible physically, with the eddy pressure $\hat{p}_I = \hat{p}_{II}$ decreasing from unity at the ends of the eddy to a negative value in the middle. Again, the numerical behaviour near the ends seems in keeping with the form $\hat{p}_I = \hat{p}_{II} = 1 + O(1-|X_*|)^3$ for $|X_*| \to 1-$, implied by (A 7), since $\hat{S} \propto (1-|X_*|)^{\frac{3}{2}}$ then.

The dependence of the mid-eddy-thickness/eddy-length ratio, and $\bar{\Omega}L$, on the Bernoulli constant C_{II} predicted from the above is

$$\frac{1}{L}(S)_{X_*=0} \sim \tfrac{1}{2}\sigma_1 C_{II}, \quad \tfrac{1}{2}\bar{\Omega}L \sim -8^{\frac{1}{4}}\sigma C_{II}^{-\frac{1}{2}} \quad \text{as } C_{II} \to 0+, \tag{A 12}$$

where σ is given in (A 11) and σ_1 is 1.702 according to our extrapolated numerical results in figure 5(*a*).

This solution for small C_{II} (large $|\bar{\Omega}L|$) tends to reinforce belief in the existence of solutions to (2.3) at $O(1)$ values of C_{II}, it may be useful in constructing such solutions computationally, and it complements Sadovskii's results obtained for values of C_{II} close to $\frac{1}{2}$. It suggests further that some parameter (e.g. C_{II}) other than Sadovskii's parameter h should be used to characterize these flows, since $h = 4(1-2C_{II})/(\bar{\Omega}L)^2$ tends to zero at both the extremes $C_{II} \to 0$ (see (A 12)) and $C_{II} \to \frac{1}{2}$. Figure 5(*b*) presents the dependence of the eddy thickness/length ratio, and $\bar{\Omega}L$, on the parameter C_{II}, according to the prediction (A 12) and to Sadovskii's four calculations. The two sets of results are fairly close, given the asymptotic nature of (A 12). Finally we observe that the governing equation (A 5) can arise in principle in the triple-deck formulation of small-scale subsonic separation eddies. So the finding of a computational solution above is an encouraging feature in that context, as it is also in the context of Prandtl–Batchelor flows where, for a thin eddy, attached to a thin body, say, (A 5) may again come into play.

REFERENCES

Acrivos, A., Leal, L. G., Snowden, D. D. & Pan, F. 1968 *J. Fluid Mech.* **34**, 25.

Batchelor, G. K. 1956 *J. Fluid Mech.* **1**, 388.

Burggraf, O. R. 1970 *Aero. Res. Lab. Rep.* 70-0275.

Elliott, J. W., Cowley, S. J. & Smith, F. T. 1983 *Geophys. Astrophys. Fluid Dyn.* **25**, 77.

Fornberg, B. 1980 *J. Fluid Mech.* **98**, 819.

Fornberg, B. 1985 *J. Comp. Phys.* (to appear).

Messiter, A. F., Hough, G. R. & Feo, A. 1973 *J. Fluid Mech.* **60**, 605.

Peregrine, D. H. 1985 *J. Fluid Mech.* (to appear).

Pierrehumbert, R. T. 1980 *J. Fluid Mech.* **99**, 129.

Riley, N. 1981 *J. Engng Maths* **15**, 15.

Sadovskii, V. S. 1971 *Prikl. Math. Mech.* **35**, 773 [transl. *Appl. Math. Mech.* **35** (1971), 729].

Smith, F. T. 1978 *RAE Tech. Rep.* TR78095.

Smith, F. T. 1979 *J. Fluid Mech.* **92**, 171.

Smith, F. T. 1981 *J. Fluid Mech.* **113**, 407.

Smith, F. T. 1983 *United Tech. Res. Center, E. Hartford, Conn., Rep.* UTRC-83-13.

Smith, F. T. 1984 *United Tech. Res. Center, E. Hartford, Conn., Rep.* UTRC-84-31.

Smith, J. H. B. 1977 *RAE Tech. Rep.* TR77058.

Sychev, V. V. 1967 *Rep. to 8th Symp. on Recent Problems in Mechanics of Liquids and Gases, Tarda, Poland.*

Sychev. V. V. 1972 *Izv. Akad. Nauk SSSR, Mekh. Zhid. Gaza* **3**, 47.

Van Dommelen, L. L. 1981 Ph.D. thesis, Cornell University.